

RESEARCH ARTICLE



Cite this: *Org. Chem. Front.*, 2026, **13**, 455

Received 10th September 2025,  
Accepted 27th October 2025

DOI: 10.1039/d5qo01292a

[rsc.li/frontiers-organic](http://rsc.li/frontiers-organic)

## Perimidine directed Rh(III)-catalyzed [4 + 1] and [4 + 2] annulations: synthesis of perimidine linked spiro-succinimides and isoquinolines

Vidya Kumari and Lokman H. Choudhury \*

We report a novel Rh(III)-catalyzed perimidine-directed C–H activation strategy for the synthesis of perimidine-fused heterocycles using various types of alkenes. The reaction of 2-aryl perimidines with maleimides in the presence of the  $[\text{RhCp}^*\text{Cl}_2]_2$  catalyst facilitates a cascade [4 + 1] spiro-annulation, affording perimidine-linked isoindoles spiro-fused with succinimides. Conversely, vinylene carbonates provided a fused six-membered ring *via* a [4 + 2] cyclization, yielding perimidine-fused isoquinolines. This methodology is useful for synthesizing a library of polycyclic perimidine-fused heterocycles.

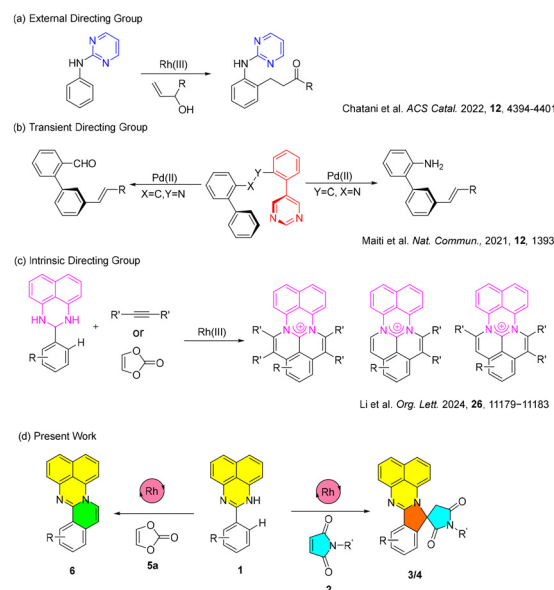
## Introduction

In modern organic synthesis, site-selective C–H activation is considered an efficient strategy for the synthesis of complex molecules. Utilizing biologically relevant scaffolds as intrinsic directing groups has gained considerable interest as it circumvents the need for installing and removing external auxiliaries, thereby providing an efficient synthetic route.<sup>1</sup>

Perimidine, a unique fused pyrimidine derivative, holds significant promise across diverse fields including medicine, life sciences, and industrial chemistry.<sup>2</sup> Perimidine derivatives demonstrate a wide spectrum of biological activities, exhibiting antimicrobial,<sup>3</sup> antibacterial,<sup>4</sup> anticancer,<sup>5</sup> antitumor,<sup>6</sup> and anti-inflammatory<sup>7</sup> properties, as well as being useful chemosensors<sup>8</sup> and coloring agents.<sup>9</sup> Perimidine exhibits distinctive electronic features arising from delocalization of the nitrogen lone pair into the naphthalene ring, imparting a unique combination of  $\pi$ -rich and  $\pi$ -deficient character that enhances its reactivity in diverse transformations.<sup>2</sup> This characteristic electronic structure enables perimidine to coordinate with metals by accepting electrons into its low-lying vacant  $\pi$ -orbitals. This coordination also enhances the electropositive character of the metal centre, thereby promoting the coordination of alkenes.<sup>10</sup>

In recent years, pyrimidine has been extensively utilized as a removable auxiliary and transient directing group for directed C–H activation.<sup>10–13</sup> In 2022, Chatani and co-workers reported the activation of the *ortho*-C–H bond of pyrimidine-protected aniline for the oxidative *ortho*-alkylation with secondary allyl alcohols to synthesize  $\beta$ -aryl ketones (eqn (a), Scheme 1).<sup>12</sup> Similarly, in 2021, Maiti and co-workers reported

*meta*-olefination of complex biaryls using a palladium catalyst and pyrimidine as a transient directing group *via* reversible imine formation (eqn (b), Scheme 1).<sup>13</sup> Despite the enormous applications in drugs and the synthetic utility of pyrimidines, using it as an intrinsic directing group is still limited. On the other hand, to the best of our knowledge, perimidine-directed C–H activation remains largely unexplored. The only related studies were reported by Li and co-workers, in which 2-aryl-2,3-dihydro-1*H*-perimidines underwent Rh(III)-catalyzed annulation to furnish cationic azaperylene derivatives (eqn (c), Scheme 1).<sup>14</sup>



**Scheme 1** Comparison of the present work with some previously reported methods.

Department of Chemistry, Indian Institute of Technology Patna, Bihta, 801106 Bihar, India. E-mail: [lokman@iitp.ac.in](mailto:lokman@iitp.ac.in), [lokman.iitp@gmail.com](mailto:lokman.iitp@gmail.com)



Furthermore, intrinsic group directed C–H annulation and spiro-annulation have gathered considerable attention recently.<sup>15–20</sup> Motivated by the directing properties of pyrimidine and the growing interest in intrinsic group-directed annulation and spiro-annulation, and in continuation of our work on C–H functionalization of heterocycles,<sup>21</sup> we turned our attention towards C–H activation using perimidine as an intrinsic directing group (eqn (d), Scheme 1). Herein, we report for the first time an efficient Rh(III)-catalyzed C–H activation strategy utilizing 2-aryl-1*H*-perimidine as an intrinsic directing group for the synthesis of structurally diverse polycyclic spiro-succinimides and isoquinoline-fused perimidines.

## Results and discussion

We initiated our study with the reaction between 2-phenyl-1*H*-perimidine (**1a**) and *N*-phenylmaleimide (**2a**) in the presence of  $[\text{RhCp}^*\text{Cl}_2]_2$  (5 mol%), NaOAc (1 equiv.), and AcOH (2 equiv.) in 1 mL of MeOH at 80 °C, which afforded the desired product **3a** in 84% yield (Table 1, entry 1). Notably, alternative C–H activation catalysts such as  $[\text{Ru}(p\text{-cymene})\text{Cl}_2]_2$ , Pd(OAc)<sub>2</sub>, and  $[\text{CoCp}^*(\text{CO})\text{I}_2]$  failed to afford the desired product (Table 1, entries 2–4). Other additives such as AgOAc and Cu(OAc)<sub>2</sub>·H<sub>2</sub>O were ineffective, with no improvement in yield (Table 1, entry 5). Subsequently, various solvents (*e.g.*, 1,2-DCE, ACN, THF, and acetone) were screened to optimize the yield (Table 1, entry 6). These results established MeOH as the most suitable solvent. Substituting AcOH with Na<sub>2</sub>CO<sub>3</sub> resulted in a decreased yield of **3a** (52%) (Table 1, entry 7). Similarly, altering the acid source was ineffective, affording a comparable yield (Table 1, entry 8). Conducting the reaction under a N<sub>2</sub>

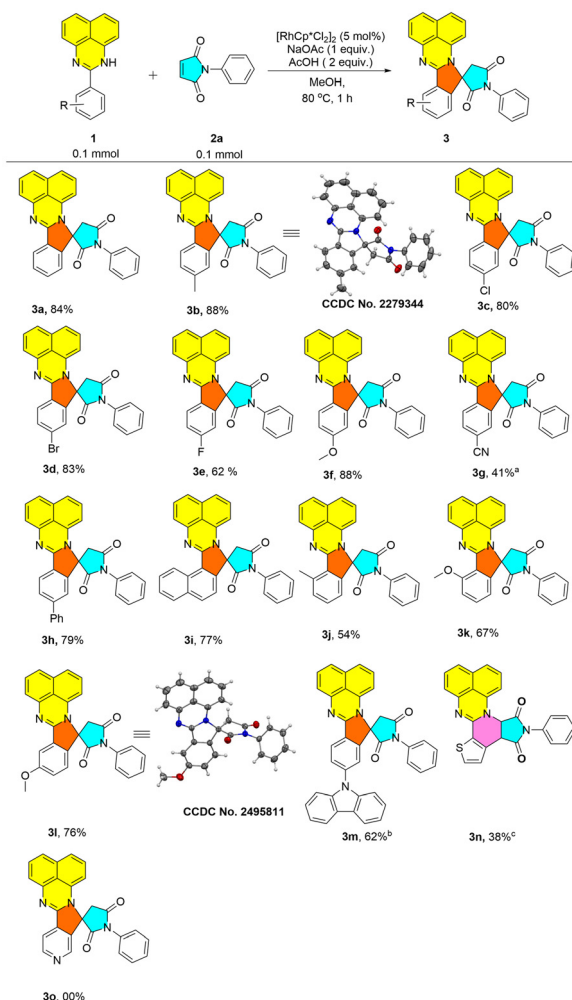
**Table 1** Optimization of reaction conditions<sup>a,b</sup>

Entry	Deviation from standard conditions	Yield <sup>b</sup>
1	None	84
2	$[\text{Ru}(p\text{-cymene})\text{Cl}_2]_2$ instead of $[\text{RhCp}^*\text{Cl}_2]_2$	NR
3	Pd(OAc) <sub>2</sub> instead of $[\text{RhCp}^*\text{Cl}_2]_2$	NR
4	$[\text{CoCp}^*(\text{CO})\text{I}_2]$ instead of $[\text{RhCp}^*\text{Cl}_2]_2$	NR
5	AgOAc/Cu(OAc) <sub>2</sub> ·H <sub>2</sub> O instead of NaOAc	65/45
6	1,2-DCE/ACN/THF/acetone instead of MeOH	43/27/ NR/55
7	Na <sub>2</sub> CO <sub>3</sub> instead of AcOH	52
8	PivOH instead of AcOH	71
9	Under N <sub>2</sub> gas	43 <sup>c</sup>
10	No $[\text{RhCp}^*\text{Cl}_2]_2$	NR
11	No NaOAc	NR
12	No AcOH	47

<sup>a</sup> Reaction conditions: **1a** (0.1 mmol), **2a** (0.1 mmol), catalyst (5 mol%), additive 1 (1.0 equiv.), and additive 2 (2.0 equiv.) in solvent (1.0 mL) at 80 °C for 1 h. <sup>b</sup> Isolated yield. <sup>c</sup> Under a N<sub>2</sub> atmosphere; 24% of **1a** was recovered; NR = no reaction.

atmosphere resulted in no improvement in yield, with 24% of the starting material remaining, suggesting that air serves as a key oxidant (Table 1, entry 9). No product formation was observed without  $[\text{RhCp}^*\text{Cl}_2]_2$  or NaOAc, while omission of AcOH led to a moderate 47% yield (Table 1, entries 10–12).

With the optimized reaction conditions established, we next explored the substrate scope by varying perimidine derivatives while keeping *N*-phenylmaleimide (**2a**) constant (Scheme 2). Under standard conditions, unsubstituted 2-phenyl-1*H*-perimidine (**1a**) reacted with *N*-phenylmaleimide (**2a**) to afford polycyclic fused succinimide **3a** in 84% yield. We then examined the effect of *para*-substitution on the phenyl ring of perimidine. Electron-donating (**1b**, **1f**) and halogen-substituted (**1c**, **1d**) compounds reacted efficiently with **2a**, affording the corresponding products in yields of 80–88%. In contrast, the fluoro-substituted derivative (**1e**) gave a reduced yield of 62%, while the strongly electron-withdrawing cyano-

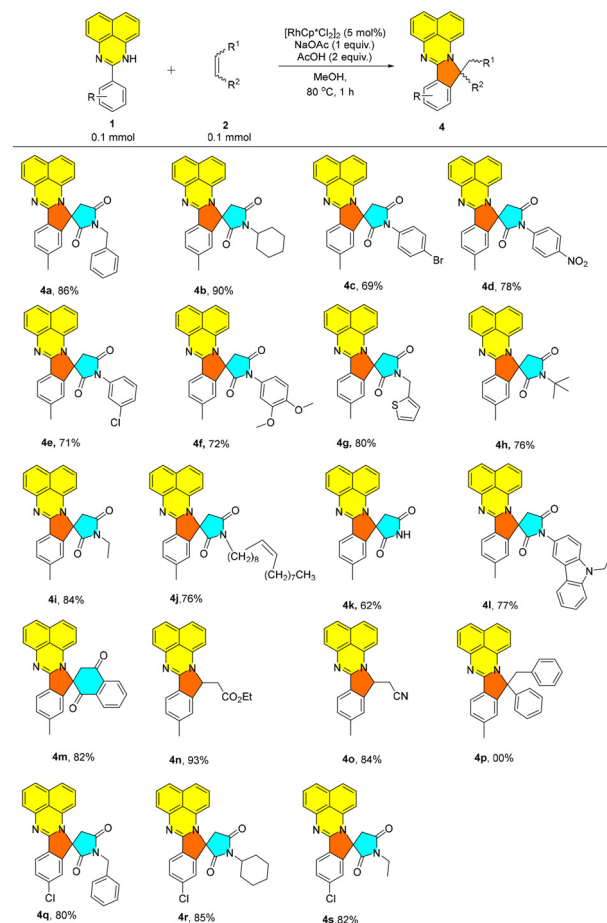


**Scheme 2** Substrate scope for 2-aryl-1*H*-perimidines. Reaction conditions: **1** (0.1 mmol), **2a** (0.1 mmol), 5 mol% (3 mg)  $[\text{RhCp}^*\text{Cl}_2]_2$ , 1.0 equiv. (8 mg) NaOAc, and 2.0 equiv. (11  $\mu\text{L}$ ) AcOH in 1.0 mL MeOH at 80 °C for 1 h; isolated yield; <sup>a</sup> 20 mol% (3 mg) AgOAc instead of 1 equiv. NaOAc for 24 h; <sup>b</sup> 6 h; <sup>c</sup> 3 h.



substituted perimidine (**1g**), *i.e.*, 4-(2,3-dihydro-1*H*-perimidin-2-yl) benzonitrile, failed to produce the desired product. So, we performed the reaction under the modified conditions using 20 mol% AgOAc instead of NaOAc; the reaction proceeded slowly to provide a low yield of the product **3g** in 24 h. The 4-phenyl-substituted perimidine (**1h**) afforded spirocyclic product **3h** in 79% yield, while naphthyl perimidine (**1i**) delivered **3i** in 77% yield. Notably, *ortho*-substituted derivatives (**1j** and **1k**) were also tolerated, furnishing **3j** and **3k** in moderate yields. All the products were fully characterized by recording <sup>1</sup>H, <sup>13</sup>C NMR and HRMS spectra. For unambiguous confirmation of the structures, the single crystal X-ray structure of the product **3b** (CCDC no. 2279344) was obtained. The crystal was grown in EtOAc as a solvent by a slow evaporation method. The details of the XRD structure of **3b** are available in the SI. In the case of *meta*-substituted perimidine **1l**, selective activation of the less hindered *ortho* C–H bond afforded product **3l** in 76% yield.<sup>15,17</sup> The structure was further confirmed by performing single crystal-XRD of **3l** (CCDC no. 2495811). The crystal was grown in EtOAc as a solvent by a slow evaporation method (for crystal details, please see the SI). The carbazole-linked perimidine **1m** also underwent smooth transformation with **2a**, delivering **3m** in 62% yield, demonstrating the protocol's compatibility with heterocycle-linked frameworks. Next, we performed the reaction with 2-(thiophen-2-yl)-1*H*-perimidine **1n** with *N*-phenylmaleimide **2a** under the standard reaction conditions. Interestingly, this reaction did not provide the desired spiro-succinimides, instead it provided the [4 + 2] annulated product **3n** in only 38% yield even after a longer reaction time (3 h), and the structure was confirmed by recording <sup>1</sup>H, <sup>13</sup>C NMR and HRMS spectra. This could be due to the slow reactivity of the 2-(thiophen-2-yl)-1*H*-perimidine **1n** towards the aza-Michael addition step. On the other hand, 2-(pyridin-4-yl)-1*H*-perimidine **1o** was found to be not suitable for this reaction and the corresponding expected product **3o** could not be prepared using this methodology.

Encouraged by these results, next, we explored the substrate scope with diverse maleimides and alkenes as summarized in Scheme 3. Perimidine **1b** reacted with *N*-benzyl (**2b**) and *N*-cyclohexyl maleimide (**2c**) to afford spirocycles **4a** and **4b** in excellent yields (86% and 90%, respectively). The 4-bromo-substituted maleimide **2d** provided **4c** in 69% yield, while the strongly electron-withdrawing 4-nitro derivative **2e** gave **4d** in a good yield of 78%. The *meta*-substituted maleimide **2f** reacted efficiently with perimidine **1b** to afford spirocycle **4e** in a good yield of 71%. Similarly, 3,4-dimethoxy-substituted maleimide **2g** gave **4f** in 72% yield. Notably, the heteroaryl-linked *N*-methyl thiophene maleimide **2h** also reacted smoothly, furnishing **4g** in 80% yield. The applicability of this methodology was further demonstrated with *N*-alkyl-substituted maleimides **2i** and **2j**, which reacted efficiently with perimidine **1b** to afford **4h** and **4i** in 76% and 84% yields, respectively. Likewise, *N*-oleyl maleimide **2k** reacted with perimidine **1b** to afford the spirocyclized product **4j** in 76% yield. The unsubstituted maleimide **2l** also reacted with **1b**, furnishing **4k** in a moderate yield of 62%. Reaction of **1b** with carbazole-linked maleimide



**Scheme 3** Substrate scope for maleimides/alkenes. Reaction condition: **1** (0.1 mmol), **2** (0.1 mmol), 5 mol% (3 mg)  $[\text{RhCp}^*\text{Cl}_2]_2$ , 1.0 equiv. (8 mg) NaOAc, and 2.0 equiv. (11  $\mu\text{L}$ ) AcOH in 1.0 mL MeOH at 80  $^\circ\text{C}$  for 1 h; Isolated Yield.

**2m** provided product **4l** in 77% yield. Naphthoquinone **2n**, a cyclic electron-deficient alkene, also afforded the [4 + 1] spirocyclized product **4m** in 82% yield. Acyclic electron-deficient alkenes like ethyl acrylate **2o** and acrylonitrile **2p** reacted with **1b** to provide [4 + 1] annulated perimidines **4n** and **4o** in excellent yields of 93% and 84%, respectively. In contrast, symmetric alkene *trans*-stilbene **2q** remained unreactive under the optimized conditions. Subsequently, 4-chlorophenyl perimidine **1c** was reacted with various maleimides, including *N*-benzyl **2b**, *N*-cyclohexyl **2c**, and *N*-ethyl **2i**. In all instances, the reaction proceeded efficiently, demonstrating the broad scope of this methodology.

After obtaining these encouraging results, we next explored vinylene carbonate as a reaction partner, replacing maleimide. Under the optimized conditions, no reaction occurred. Consequently, we optimized reaction conditions for the reaction of 2-phenyl-1*H*-perimidine **1a** with vinylene carbonate **5a**. After a series of reactions (summarized in Table 2), we found that vinylene carbonates can be reacted with **1a**. Interestingly, the resulting product is a fused six-membered ring formed *via*



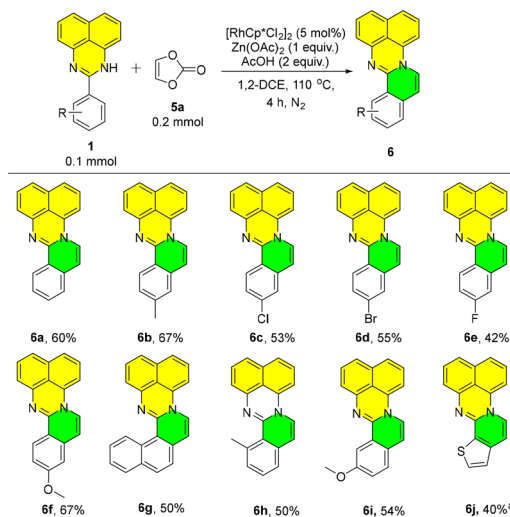
Table 2 Optimization of reaction conditions<sup>a,b</sup>

Entry	Deviation from standard conditions	Yield <sup>b</sup>
1	None	60
2	AgSbF <sub>6</sub> /AgOTf/AgNTf <sub>2</sub> /KPF <sub>6</sub> /NaOAc <sup>c</sup> Instead of Zn(OAc) <sub>2</sub>	45/45/41/30/trace
3	Toluene/DCM/ACN instead of 1,2-DCE	41/37/22
4	80 °C/130 °C instead of 110 °C	41/45
5	Air instead of N <sub>2</sub> gas	Trace
6	No [RhCp*Cl <sub>2</sub> ] <sub>2</sub>	NR
7	No Zn(OAc) <sub>2</sub>	NR
8	No AcOH	30

<sup>a</sup> Reaction conditions: **1a** (0.1 mmol), **5a** (0.2 mmol), catalyst (5 mol%), additive 1 (1.0 equiv.), and additive 2 (2.0 equiv.) in solvent (1.0 mL) at 110 °C for 4 h under N<sub>2</sub>. <sup>b</sup> Isolated yield. <sup>c</sup> MeOH instead of 1,2-DCE; NR = no reaction.

a [4 + 2] annulation. Among all the screened conditions, entry 1 conditions in Table 2 provided the best result and were therefore considered the optimal reaction conditions.

After establishing the optimal conditions, next we studied the generality of this methodology, and the results are summarized in Scheme 4. We initially reacted 2-phenyl-1*H*-perimidine (**1a**) with vinylene carbonate (**5a**) under the optimal conditions, yielding product **6a** in 60%. Subsequent reactions with *para*-substituted perimidines (**1a–1f**) generally gave good yields, except for the 4-fluoro derivative (**1e**), which produced **6e** in only 42% yield under the standard conditions. We then treated naphthyl-1*H*-perimidine (**1i**) with vinylene carbonate



**Scheme 4** Substrate scope of vinylene carbonates. Reaction conditions: **1** (0.1 mmol), **5a** (0.2 mmol), 5 mol% (3 mg) of [RhCp\*Cl<sub>2</sub>]<sub>2</sub>, 1.0 equiv. (18 mg) of Zn(OAc)<sub>2</sub>, and 2.0 equiv. (11  $\mu$ L) of AcOH in 1.0 mL of 1,2-DCE at 110 °C for 4 h under N<sub>2</sub>; isolated yield; <sup>a</sup> 6 h.

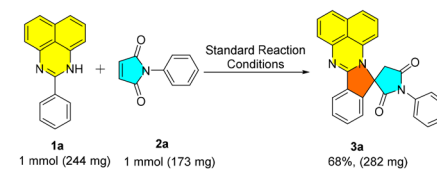
(**5a**), yielding 50% of the [4 + 2] cyclized product **6g**. The substituent at the *ortho* position of 2-phenyl-1*H*-perimidine provided **6h** in a moderate yield of 50%, whereas the *meta* substituted perimidine resulted in the selective activation of the less hindered C–H bond, furnishing a 54% yield of **6i**.<sup>15,17</sup> Next, we treated the heteroaromatic 2-(thiophen-2-yl)-1*H*-perimidine **1n**. The reaction proceeded to furnish the [4 + 2] annulated product **6j** in 6 h.

To demonstrate scalability, the reaction was performed on a 1 mmol scale with perimidine (**1a**) and *N*-phenylmaleimide (**2a**), providing 68% yield of compound **3a** under standard conditions as shown in Scheme 5.

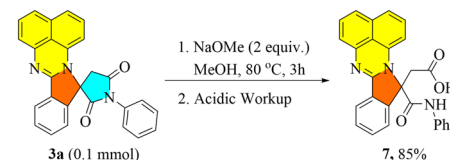
Subsequently, to illustrate late-stage modifications, an additional reaction was carried out using the reported method as shown in Scheme 6.<sup>22</sup> We conducted a ring-opening reaction of spiro-succinimide **3a** with NaOMe, followed by acid work-up yielding product **7** in 85% yield.

To understand the mechanism, we conducted a few control experiments (Scheme 7). Reacting **1e** and **1f** (1:1) with *N*-phenyl maleimide **2a** under standard conditions (eqn (a), Scheme 7) yielded **3e** and **3f** in a 1:1.3 ratio, suggesting an electrophilic cyclo-rhodation. The deuterium exchange with perimidine **1f** under the optimum reaction conditions for [4 + 1] and [4 + 2] cyclizations resulted in 25% and 78% deuteration, respectively, at both the *ortho* positions, suggesting a reversible C–H activation (eqn (b), Scheme 7).<sup>23,24</sup> The radical trapping experiment with 2 equivalents of BHT under standard reaction conditions proceeded without any significant abatement of yield, *i.e.*, 72% and 48%, respectively, ruling out the probability of any radical being involved in the reaction pathway (eqn (c), Scheme 7). The competitive kinetic isotope effect studies afforded  $k_H/k_D$  values of 2.70 and 5.25, respectively, in both cases. This delineates that C–H bond breaking is involved in the rate-determining step (eqn (d) and (e), Scheme 7).

On the basis of our control experiments and previously reported studies<sup>25–32</sup> and the obtained mass spectra, we have proposed a plausible mechanism accounting for the cascade

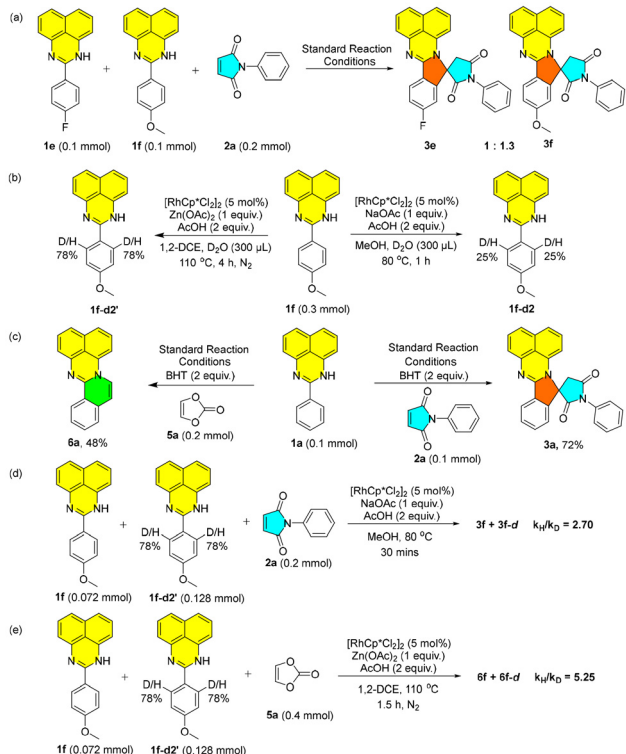


**Scheme 5** 1 mmol scale synthesis of **3a**.



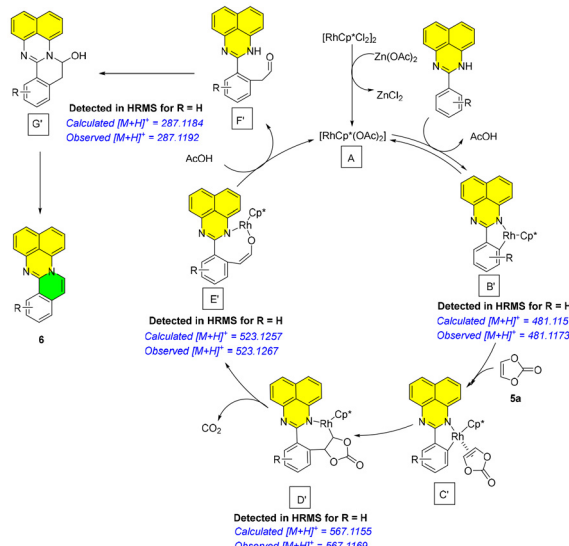
**Scheme 6** Late-stage modification of **3a**.





Scheme 7 Control experiments.

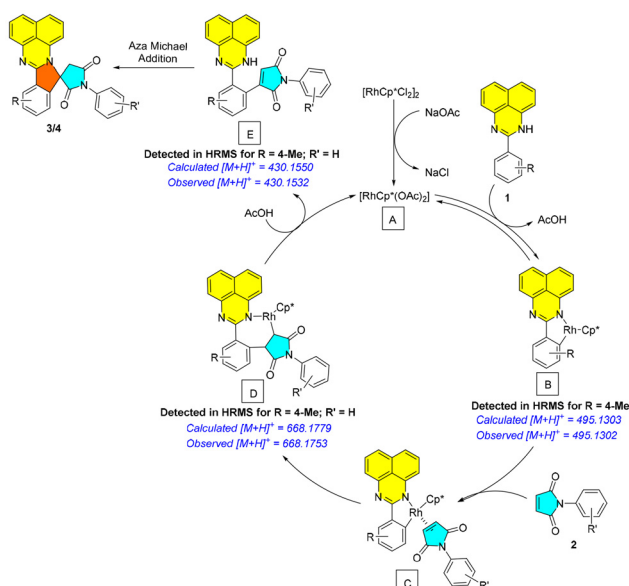
annulations (Schemes 8 and 9). Initially, the  $[\text{RhCp}^*\text{Cl}_2]_2$  is activated upon reaction with NaOAc, resulting in the monomeric active catalyst  $[\text{RhCp}^*(\text{OAc})_2]$  A, which undergoes reversible C–H activation with 2-aryl-1*H*-perimidine, leading to the formation of intermediate B. The maleimide 2 then coordinates with B, yielding complex C, which, upon migratory insertion, forms the seven-membered rhodacycle D. A  $\beta$ -hydride elimination generates the alkenylated intermediate E along with regeneration of the active catalyst A. Intermediate E then undergoes a rapid aza-Michael addition to form the spiro-annulated product 3/4.



Scheme 9 Plausible reaction mechanism for 6.

In the catalytic cycle with vinylene carbonate (Scheme 9),  $[\text{RhCp}^*\text{Cl}_2]_2$  is activated by  $\text{Zn}(\text{OAc})_2$  to form monomeric Rh(III) complex A followed by C–H activation with 2-aryl-1*H*-perimidine to form rhodacycle B'. Coordination with vinylene carbonate 5a forms complex C', which undergoes migratory insertion to yield the seven-membered intermediate D'. A  $\beta$ -oxygen elimination and decarboxylation from D' generates the eight-membered ring E'. The intermediate E' undergoes protonation with AcOH, producing intermediate F' and regenerates the active catalyst A. Intermediate F' undergoes intramolecular cyclization and dehydration to afford the [4 + 2] cyclized product 6.

In the catalytic cycle with vinylene carbonate (Scheme 9),  $[\text{RhCp}^*\text{Cl}_2]_2$  is activated by  $\text{Zn}(\text{OAc})_2$  to form monomeric Rh(III) complex A followed by C–H activation with 2-aryl-1*H*-perimidine to form rhodacycle B'. Coordination with vinylene carbonate 5a forms complex C', which undergoes migratory insertion to yield the seven-membered intermediate D'. A  $\beta$ -oxygen elimination and decarboxylation from D' generates the eight-membered ring E'. The intermediate E' undergoes protonation with AcOH, producing intermediate F' and regenerates the active catalyst A. Intermediate F' undergoes intramolecular cyclization and dehydration to afford the [4 + 2] cyclized product 6.



Scheme 8 Plausible reaction mechanism for 3/4.

## Author contributions

Vidya Kumari: concept building, performing experiments, data acquisition, data analysis and manuscript writing. Lokman H. Choudhury: concept building, supervision, fund acquisition and manuscript writing.

## Conflicts of interest

The authors declare no conflicts of interest.

## Data availability

The data supporting this article have been included in the manuscript and its supplementary information (SI). Supplementary information is available. See DOI: <https://doi.org/10.1039/d5qo01292a>.

CCDC 2279344 and 2495811 contain the supplementary crystallographic data for this paper.<sup>33a,b</sup>

## Acknowledgements

L. H. C. gratefully acknowledges the financial support from the ANRF, Government of India (Sanction No. CRG/2021/003716). The authors also express their sincere gratitude to IIT Patna for providing essential research facilities, and to SAIF IIT Patna, IIT (ISM) Dhanbad and BHU, Varanasi, for NMR, HRMS and SC-XRD analyses. Special thanks are extended to Mr Kamlesh Satpute (IIT Ropar) for his assistance with single-crystal X-ray diffraction analysis.

## References

- 1 (a) G. Meng, N. Y. S. Lam, E. L. Lucas, T. G. Saint-Denis, P. Verma, N. Chekshin and J. Q. Yu, Achieving Site-Selectivity for C–H Activation Processes Based on Distance and Geometry: A Carpenter’s Approach, *J. Am. Chem. Soc.*, 2020, **142**, 10571–10591; (b) L. Zhang and T. Ritter, A Perspective on Late-Stage Aromatic C–H Bond Functionalization, *J. Am. Chem. Soc.*, 2022, **144**, 2399–2414; (c) C. M. Josephitis, H. M. Nguyen and A. McNally, Late-Stage C–H Functionalization of Azines, *Chem. Rev.*, 2023, **123**, 7655–7691; (d) Y. Wang, S. Dana, H. Long, Y. Xu, Y. Li, N. Kaplaneris and L. Ackermann, Electrochemical Late-Stage Functionalization, *Chem. Rev.*, 2023, **123**, 11269–11335.
- 2 N. Sahiba and S. Agarwal, Recent Advances in the Synthesis of Perimidines and Their Applications, *Top. Curr. Chem.*, 2020, **378**, 44.
- 3 M. Azam, I. Warad, S. I. Al-Resayes, N. Alzaqri, M. R. Khan, R. Pallepogu, S. Dwivedi, J. Musarrat and M. Shakir, Synthesis and Structural Characterization of Pd(II) Complexes Derived from Perimidine Ligand and Their *in vitro* Antimicrobial Studies, *J. Mol. Struct.*, 2013, **1047**, 48–54.
- 4 T. A. Farghaly and H. K. Mahmoud, Site-and Regioselectivity of the Reaction of Hydrazonoyl Chlorides with Perimidine Ketene Aminal. Antimicrobial Evaluation of the Products, *J. Heterocycl. Chem.*, 2015, **52**, 86–91.
- 5 H. A. Eldeab and A. F. A. Eweas, A Greener Approach Synthesis and Docking Studies of Perimidine Derivatives as Potential Anticancer Agents, *J. Heterocycl. Chem.*, 2018, **55**, 431–439.
- 6 T. A. Farghaly, E. M. Abbas, K. M. Dawood and T. B. El-Naggar, Synthesis of 2-phenylazonaphtho [1,8-ef][1,4] diazepines and 9-(3-arylhydrazono)pyrrolo[1,2-*a*] Perimidines as Antitumor Agents, *Molecules*, 2014, **19**, 740–755.
- 7 F. A. Bassyouni, S. M. Abu-Bakr, K. H. Hegab, W. El-Eraky, A. A. El Beih and M. E. A. Rehim, Synthesis of New Transition Metal Complexes of 1H-perimidine Derivatives Having Antimicrobial and Anti-Inflammatory Activities, *Res. Chem. Intermed.*, 2012, **38**, 1527–1550.
- 8 N. Chakraborty, S. Banik, A. Chakraborty, S. K. Bhattacharya and S. Das, Synthesis of a Novel Pyrene Derived Perimidine and Exploration of its Aggregation Induced Emission, Aqueous Copper Ion Sensing, Effective Antioxidant and BSA Interaction Properties, *J. Photochem. Photobiol. A*, 2019, **377**, 236–246.
- 9 P. Kalle, M. A. Kiseleva, S. V. Tatarin, D. E. Smirnov, A. Y. Zakharov, V. V. Emets, A. V. Churakov and S. I. Bezzubov, A Panchromatic Cyclometalated Iridium Dye Based on 2-Thienyl-perimidine, *Molecules*, 2022, **27**, 3201.
- 10 S. Bag, K. Surya, A. Mondal, R. Jayarajan, U. Dutta, S. Porey, R. B. Sunoj and D. Maiti, Palladium-Catalyzed *meta*-C–H Allylation of Arenes: A Unique Combination of a Pyrimidine-Based Template and Hexafluoroisopropanol, *J. Am. Chem. Soc.*, 2020, **142**, 12453–12466.
- 11 (a) J. A. Leitch, C. L. McMullin, A. J. Paterson, M. F. Mahon, Y. Bhonoah and C. G. Frost, Ruthenium–Catalyzed *para*-Selective C–H Alkylation of Aniline Derivatives, *Angew. Chem., Int. Ed.*, 2017, **56**, 15131–15135; (b) S. Bag, R. Jayarajan, U. Dutta, R. Chowdhury, R. Mondal and D. Maiti, Remote *meta*-C–H Cyanation of Arenes Enabled by a Pyrimidine-Based Auxiliary, *Angew. Chem., Int. Ed.*, 2017, **56**, 12538–12542; (c) T. K. Achar, X. Zhang, R. Mondal, M. S. Shanavas, S. Maiti, S. Maity, N. Pal, R. S. Paton and D. Maiti, Palladium–Catalyzed Directed *meta*-Selective C–H Allylation of Arenes: Unactivated Internal Olefins as Allyl Surrogates, *Angew. Chem.*, 2019, **131**, 10461–10468; (d) S. M. Khake and N. Chatani, The Direct Rh(III)-Catalyzed C–H Amidation of Aniline Derivatives Using a Pyrimidine Directing Group: The Selective Solvent Controlled Synthesis of 1,2-Diaminobenzenes and Benzimidazoles, *Org. Lett.*, 2020, **22**, 3655–3660.
- 12 S. M. Khake and N. Chatani, Rhodium(III)-Catalyzed Oxidative C–H Alkylation of Aniline Derivatives with Allylic Alcohols to Produce  $\beta$ -Aryl Ketones, *ACS Catal.*, 2022, **12**, 4394–4401.



13 S. Bag, S. Jana, S. Pradhan, S. Bhowmick, N. Goswami, S. K. Sinha and D. Maiti, Imine as a Linchpin Approach for *meta*-C–H Functionalization, *Nat. Commun.*, 2021, **12**, 1393.

14 (a) H. Li, Y. Zeng, F. Liang, Y. Yang, K. Li, F. Pang and S. Li, Programmable Synthesis of Cationic Azaperylenes via Rh (III)-Catalyzed Multiple C–H/N–H Bonds Activation and Annulation, *Org. Lett.*, 2024, **26**, 11179–11183; (b) Y. Zeng, H. Li, F. Liang and S. Li, Nitrogen Source-Tailored Multicomponent C–H Di/Triannulation of  $\alpha$ -Oxocarboxylic Acids and Alkynes to Diverse Cationic N-Doped PAHs, *ACS Catal.*, 2025, **15**, 12094–12102.

15 B. Hu, G. Chen, J. Zhao, L. Xue, Y. Jiang, X. Zhang and X. Fan, Synthesis of Succinimide Spiro-Fused Sultams from the Reaction of N-(Phenylsulfonyl)acetamides with Maleimides via C (sp<sup>2</sup>)-H Activation, *J. Org. Chem.*, 2021, **86**, 10330–10342.

16 N. Li, B. Hu, X. Zhang and X. Fan, Selective Construction of Spiro or Fused Heterocyclic Scaffolds via One-Pot Cascade Reactions of 1-Arylpyrazolidinones with Maleimides, *J. Org. Chem.*, 2023, **88**, 60–74.

17 W. Y. Pu, X. Y. Chen and L. Dong, Rh(III)-Catalyzed [5 + 1] Spirocyclization to Produce Novel Benzimidazole-incorporated Spirosuccinimides, *Green Synth. Catal.*, 2023, **4**, 338–341.

18 Q. Zhou, B. Li, X. Zhang and X. Fan, C–H Activation-Initiated Spiroannulation Reactions and Their Applications in the Synthesis of Spirocyclic Compounds, *Org. Biomol. Chem.*, 2024, **22**, 2324–2338.

19 R. N. Patel, D. M. Patel, D. G. Thakur, N. B. Rathod, S. D. Patel, M. A. Sonawane and S. C. Ghosh, Synthesis of Benzo [d,e] Quinoline-Spiro-Succinimides via Rhodium-Catalyzed C–H Activation/Annulation of 1-Naphthylamides with Maleimides, *Org. Biomol. Chem.*, 2025, **23**, 6897–6902.

20 C. Yang, B. Li, P. Shi, H. Xu, X. Zhang and X. Fan, Synthesis of Benzoisochromene Derivatives via C–H Activation-Initiated Cascade Formal [4 + 2] and [2 + 4] Annulation of Aryl Enaminone with Vinyl-1,3-dioxolan-2-one, *Org. Lett.*, 2025, **27**, 2964–2969.

21 (a) D. Ali, N. Mondal and L. H. Choudhury, I<sub>2</sub>/PIDA Mediated Regioselective Metal-Free Synthesis of Aryl Selenoether-Linked Trisubstituted Thiazoles, *J. Org. Chem.*, 2025, **90**, 8903–8916; (b) V. Kumari, S. S. Acharya, N. Mondal and L. H. Choudhury, Maleimide-Dependent Rh(III)-Catalyzed Site-Selective Mono and Dual C–H Functionalization of 2-Arylbenzo[d]thiazole and Oxazole Derivatives, *J. Org. Chem.*, 2024, **89**, 18003–18018.

22 A. K. Gola, A. Dubey and S. K. Pandey, Mn(I)-Catalyzed Site-Selective C–H Activation: Unlocking Access to 3-Arylated Succinimides from 2-Arylpyridines and Maleimides, *J. Org. Chem.*, 2024, **89**, 15020–15025.

23 D. H. Dethé, V. Kumar and R. Das, Ru(II)-Catalyzed C–H Activation/[4 + 2] Annulation of Sulfoxonium Ylide with Maleimide: Access to Fused Benzo[e]isoindole-1,3,5-trione, *Org. Lett.*, 2024, **26**, 6830–6834.

24 (a) A. Mandal, S. Dana, H. Sahoo, G. S. Grandhi and M. Baidya, Ruthenium(II)-catalyzed *ortho*-C–H Chalcogenation of Benzoic Acids via Weak O-Coordination: Synthesis of Chalcogenoxanthones, *Org. Lett.*, 2017, **19**, 2430–2433; (b) Z. J. Zhang, M. M. Simon, S. Yu, S. W. Li, X. Chen, S. Cattani, X. Hong and L. Ackermann, Nickel-Catalyzed Atroposelective C–H Alkylation Enabled by Bimetallic Catalysis with Air-Stable Heteroatom-Substituted Secondary Phosphine Oxide Preligands, *J. Am. Chem. Soc.*, 2024, **146**, 9172–9180; (c) S. Devkota, H. J. Lee, S. H. Kim and Y. R. Lee, Direct Construction of Diverse Polyheterocycles Bearing Pyrrolidinediones via Rh(II)-Catalyzed Cascade C–H Activation/Spirocyclization, *Adv. Synth. Catal.*, 2019, **361**, 5587–5595.

25 M. Aslam, S. Mohandoss and Y. R. Lee, Chemoselective Installation of Diverse Succinimides on Fused Benzimidazoles via Rhodium-Catalyzed C–H Activation/Annulation: Chemosensor for Heavy Metals, *Org. Lett.*, 2021, **23**, 6206–6211.

26 K. Seal and B. Banerji, Ru(II) Catalyzed Oxidative Dehydrogenative Annulation and Spirocyclization of Isoquinolones with N-Substituted Maleimides, *Adv. Synth. Catal.*, 2024, **366**, 1788–1808.

27 J. Y. Kang, W. An, S. Kim, N. Y. Kwon, T. Jeong, P. Ghosh, H. S. Kim, N. K. Mishra and I. S. Kim, Synthesis of Spirosuccinimides via Annulative Cyclization Between N-Aryl Indazolols and Maleimides Under Rhodium(III) Catalysis, *Chem. Commun.*, 2021, **57**, 10947–10950.

28 K. Ghosh, Y. Nishii and M. Miura, Rhodium-Catalyzed Annulative Coupling Using Vinylene Carbonate as an Oxidizing Acetylene Surrogate, *ACS Catal.*, 2019, **9**, 11455–11460.

29 L. Wang, K. C. Jiang, N. Zhang and Z. H. Zhang, Rhodium-Catalyzed Synthesis of Isoquinolino [1,2-*b*] Quinazolines via C–H Annulation in Biomass-Derived  $\gamma$ -Valerolactone, *Asian J. Org. Chem.*, 2021, **10**, 1671–1674.

30 M. Kato, K. Ghosh, Y. Nishii and M. Miura, Rhodium-Catalysed Direct Formylmethylation using Vinylene Carbonate and Sequential Dehydrogenative Esterification, *Chem. Commun.*, 2021, **57**, 8280–8283.

31 Z. H. Wang, H. Wang, H. Wang, L. Li and M. D. Zhou, Ruthenium(II)-Catalyzed C–C/C–N Coupling of 2-arylquinazolinones with Vinylene Carbonate: Access to Fused Quinazolinones, *Org. Lett.*, 2021, **23**, 995–999.

32 G. Huang, J. T. Yu and C. Pan, Rhodium-Catalyzed C–H Activation/Annulation of N-Aryl-pyrazolidinones with Vinylene Carbonate, *Eur. J. Org. Chem.*, 2022, e202200279.

33 (a) CCDC 2279344: Experimental Crystal Structure Determination, 2025, DOI: [10.5517/ccdc.csd.cc2ghv72](https://doi.org/10.5517/ccdc.csd.cc2ghv72); (b) CCDC 2495811: Experimental Crystal Structure Determination, 2025, DOI: [10.5517/ccdc.csd.cc2ps31n](https://doi.org/10.5517/ccdc.csd.cc2ps31n).

